Supplementary information

A fat-tissue sensor couples growth to oxygen availability by remotely controlling insulin secretion

Texada, *et al.*

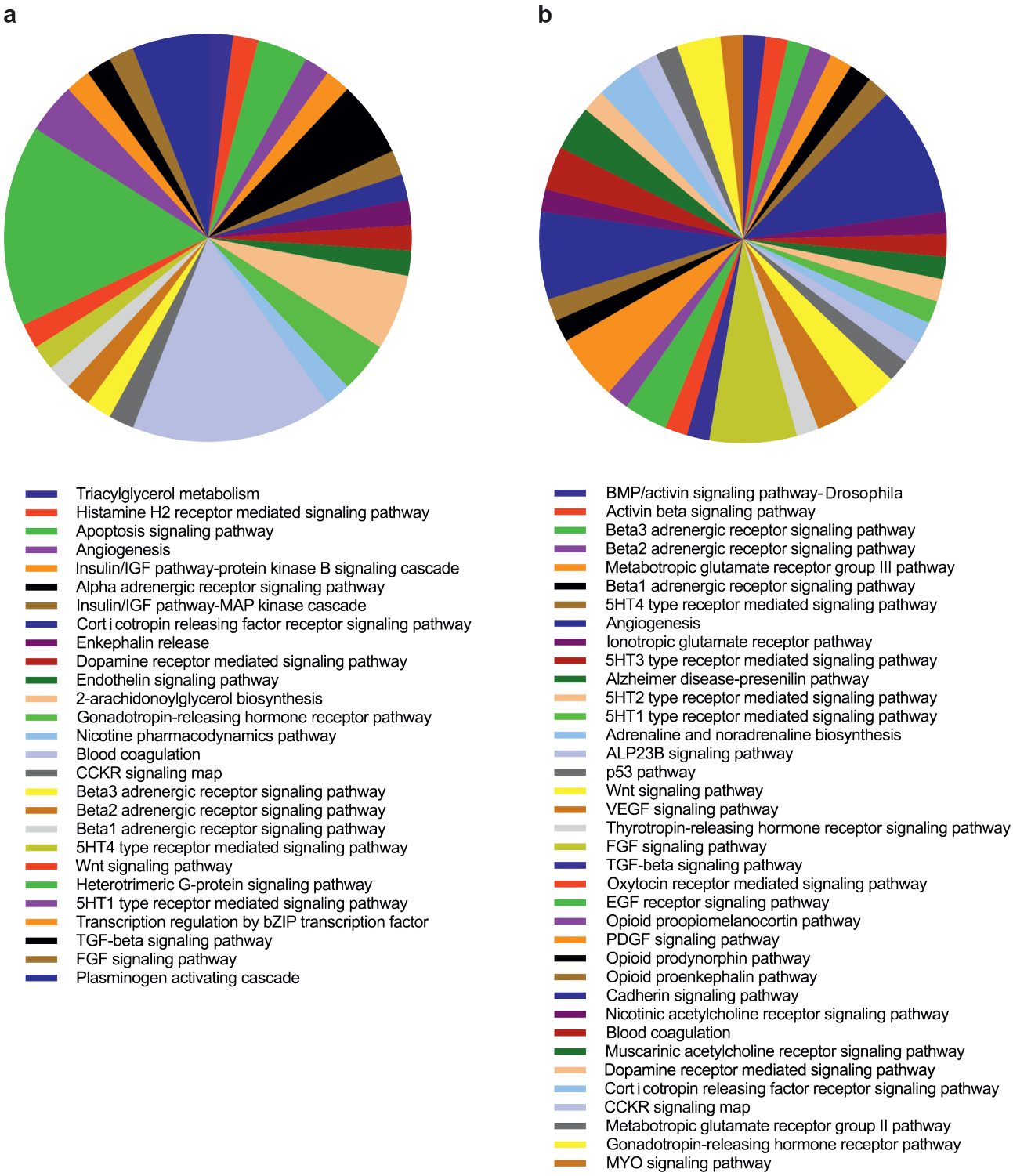

Supplementary Fig. 1. a-b Gene-ontology (GO) analysis of hits from the RNAi screen whose knockdown is associated with increased (**a**) or decreased (**b**) pupal size. Underlying data are provided in the Source Data file.

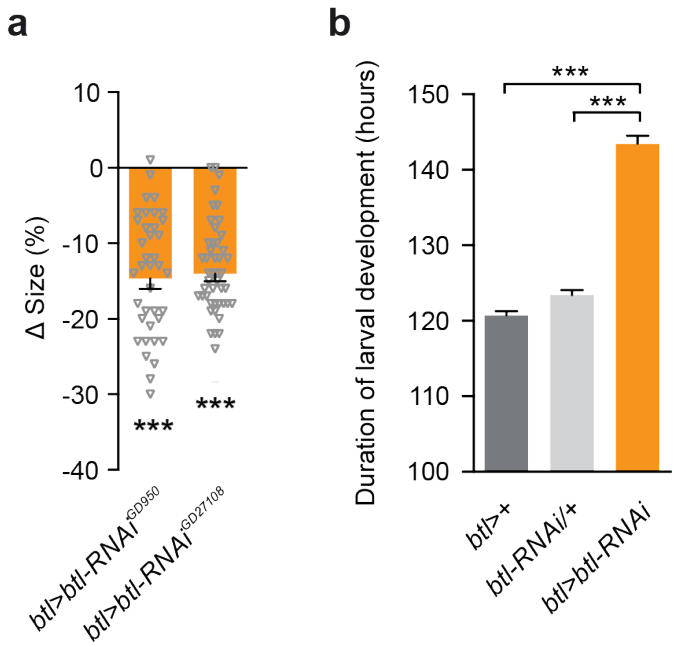

Supplementary Fig. 2. a Knockdown of *breathless* (*btl*) in the tracheae (*btl>btl-RNAi*) with two additional RNAi lines from VDRC (transformant ID numbers 950 and 27108) targeting independent sequences of *btl* reduces pupal body size compared to the control (*btl>* crossed to wild type, w^{1118}). *n* = 39-48. **b** Duration of larval development determined by the onset of pupariation of animals with trachea-specific *btl* knockdown compared to *btl>+* driver (*btl>* crossed to wild type, w^{1118}) and *btl-RNAi/+* (*btl-RNAi* crossed to wild type, w^{1118}) controls. *n* = 46-69. Statistics: one-way ANOVA with Dunnett's multiple-comparisons test. ***P<0.001, compared to the control. Error bars indicate standard error of the mean (SEM). Underlying data are provided in the Source Data file.

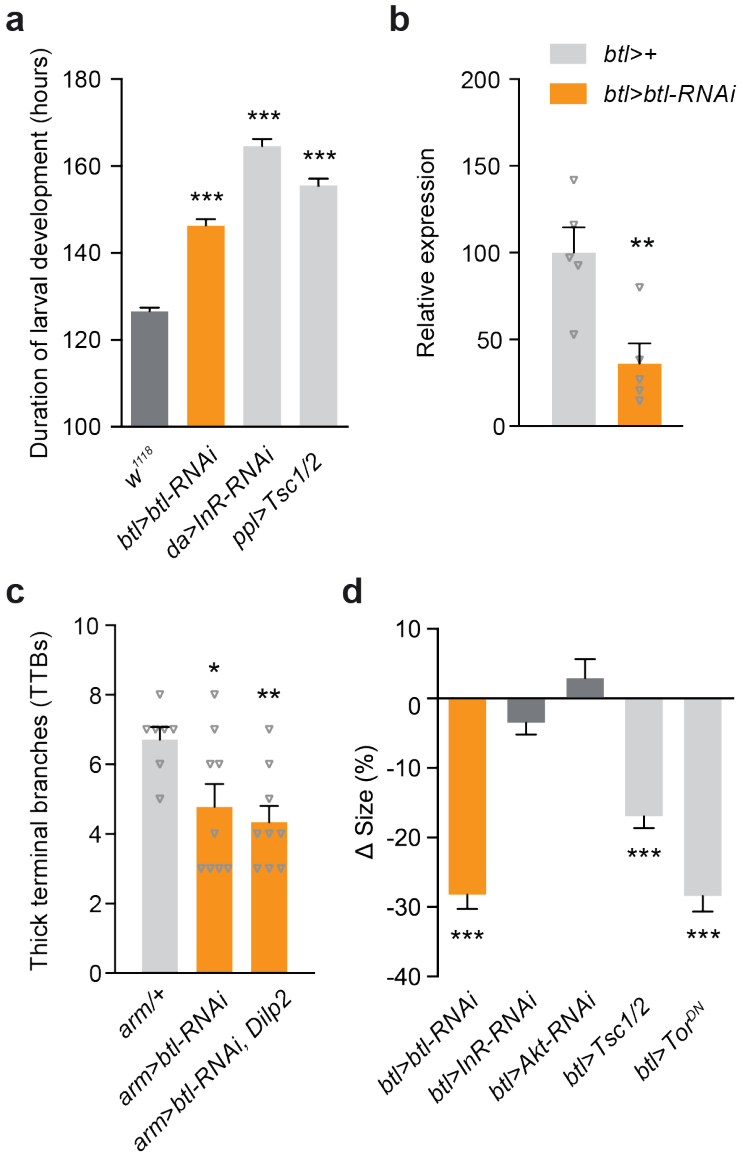

Supplementary Fig. 3. a Duration of larval development determined by the onset of pupariation of *da>InR-RNAi* animals with global knockdown of the insulin receptor (*InR*), and *ppl>Tsc1/2* animals with fat-body-specific Tor inhibition compared to controls (w^{1118}). n = 60-74. **b** Transcript levels of the ecdysone-inducible *E75B* gene. n = 5. **c** Effect of global *btl* knockdown and *Dilp2* overexpression using the weak ubiquitous *arm>* driver on the number of thick terminal branches (TTBs) per terminal cell, quantified as the number of cell projections. n = 7-9. **d** Pupal size changes in animals with trachea-specific loss of *breathless* (*btl*) (*btl>btl-RNAi*), insulin signal transduction (*btl>InR-RNAi* and *btl>Akt-RNAi*), or Tor signaling (*btl>Tsc1/2* and *btl>*Tor^{DN}) compared to *btl>+* controls (*btl>* crossed to wild type, w^{1118}). n = 22-79. Statistics: one-way ANOVA with Dunnett's test for multiple comparisons and Student's t-test for pairwise comparisons. *P<0.05, **P<0.01, ***P<0.001, compared to the control. Error bars indicate standard error of the mean (SEM). Underlying data are provided in the Source Data file.

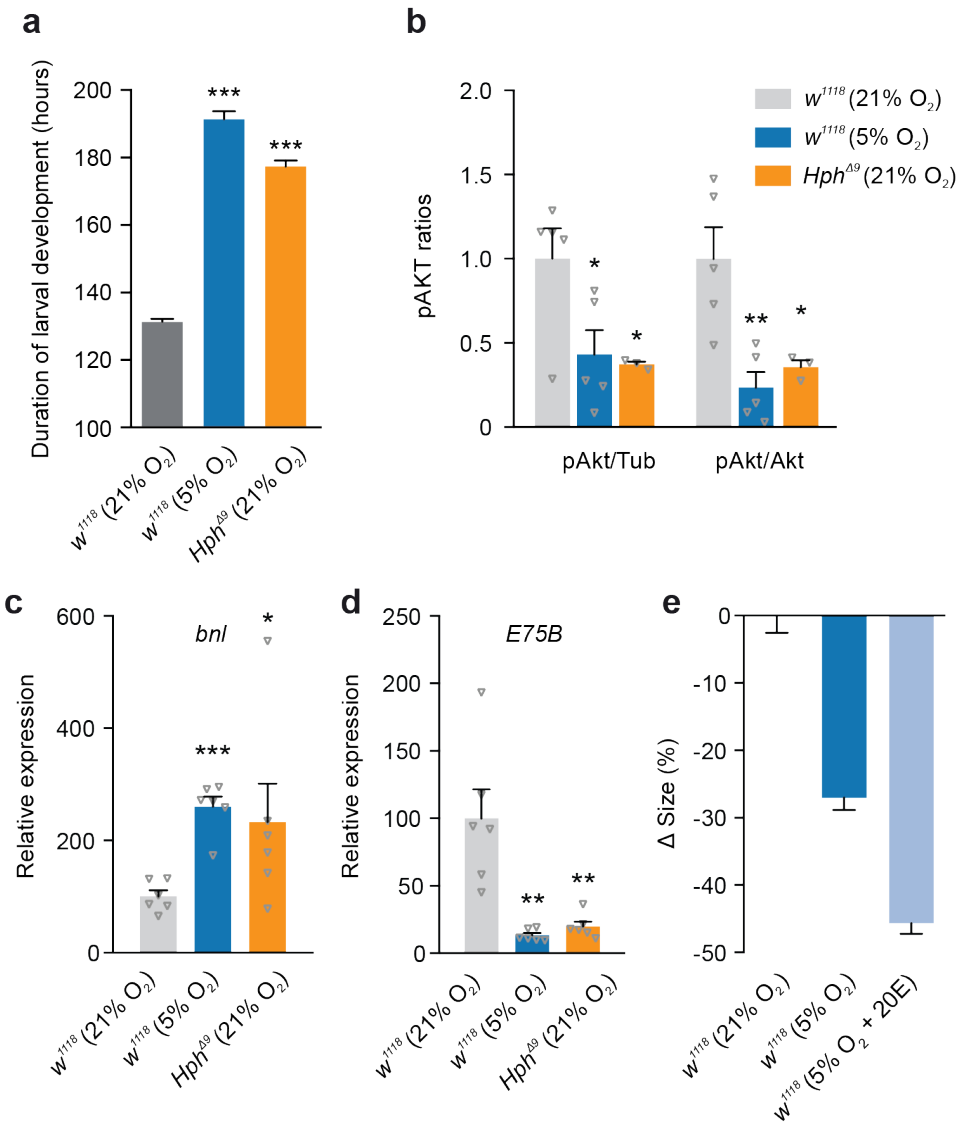

Supplementary Fig. 4. a Duration of larval development determined by the onset of pupariation of wild-type (w^{1118}) animals under normoxia (21% O_2) and hypoxia (5% O_2), and *Hph* mutant animals under normoxia. n = 57-73. **b** Whole-animal levels of phosphorylated Akt (pAkt) kinase determined by immunoblotting in normoxia (21% O_2) and hypoxia (5% O_2), and *Hph* mutant animals normalized to alpha-Tubulin (Tub) or Akt levels. n = 3-5. **c-d** Transcript levels of *branchless* (*bnl*) (**c**) and ecdysone-inducible gene *E75B* (**d**) in whole larvae under normoxia in wild-types and *Hph* mutants and in wild-types under hypoxic conditions. n = 6. **e** Effects of 20-hydroxyecdysone (20E) feeding on pupal size of wild type (w^{1118}) animals under hypoxia. n = 27-29. Statistics: one-way ANOVA with Dunnett's multiple-comparisons test. *P<0.05, **P<0.01, ***P<0.001, compared to the control. Error bars indicate standard error of the mean (SEM). Underlying data are provided in the Source Data file.

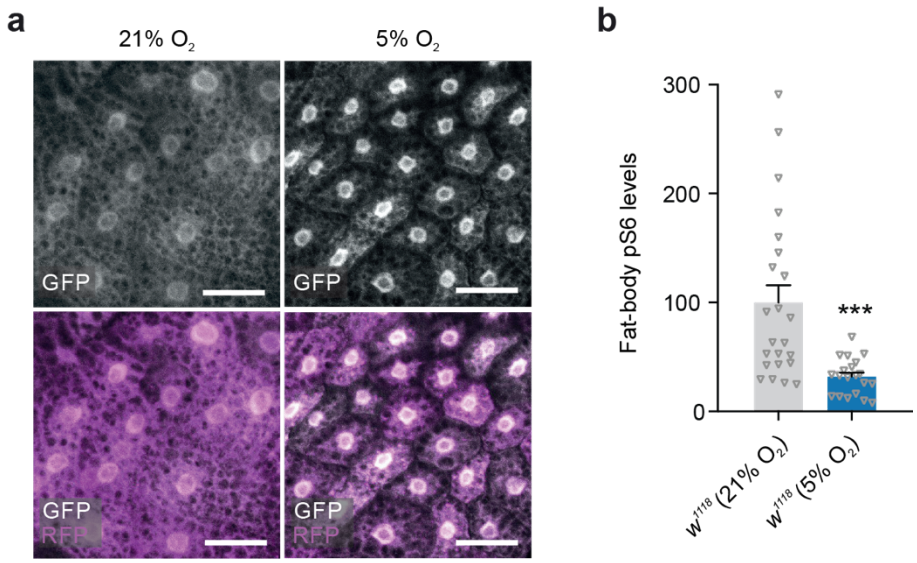

Supplementary Fig. 5. a Transgenic GFP::ODD (white) and RFP (magenta) reporter of hypoxia indicates that the fat body experiences low oxygen levels that inhibit Hph (increased GFP) when wild-type (w^{1118}) animals are incubated under 5% O_2 compared to 21% O_2 conditions. Scale bar, 20 µm. **b** Fat-body phosphorylated ribosomal protein S6 (anti-pS6) levels are reduced in larvae reared under hypoxia (5% O_2). *n* = 20-23. Statistics: Student's t-test for pairwise comparisons. ***P<0.001, compared to the control. Error bars indicate standard error of the mean (SEM). Underlying data are provided in the Source Data file.

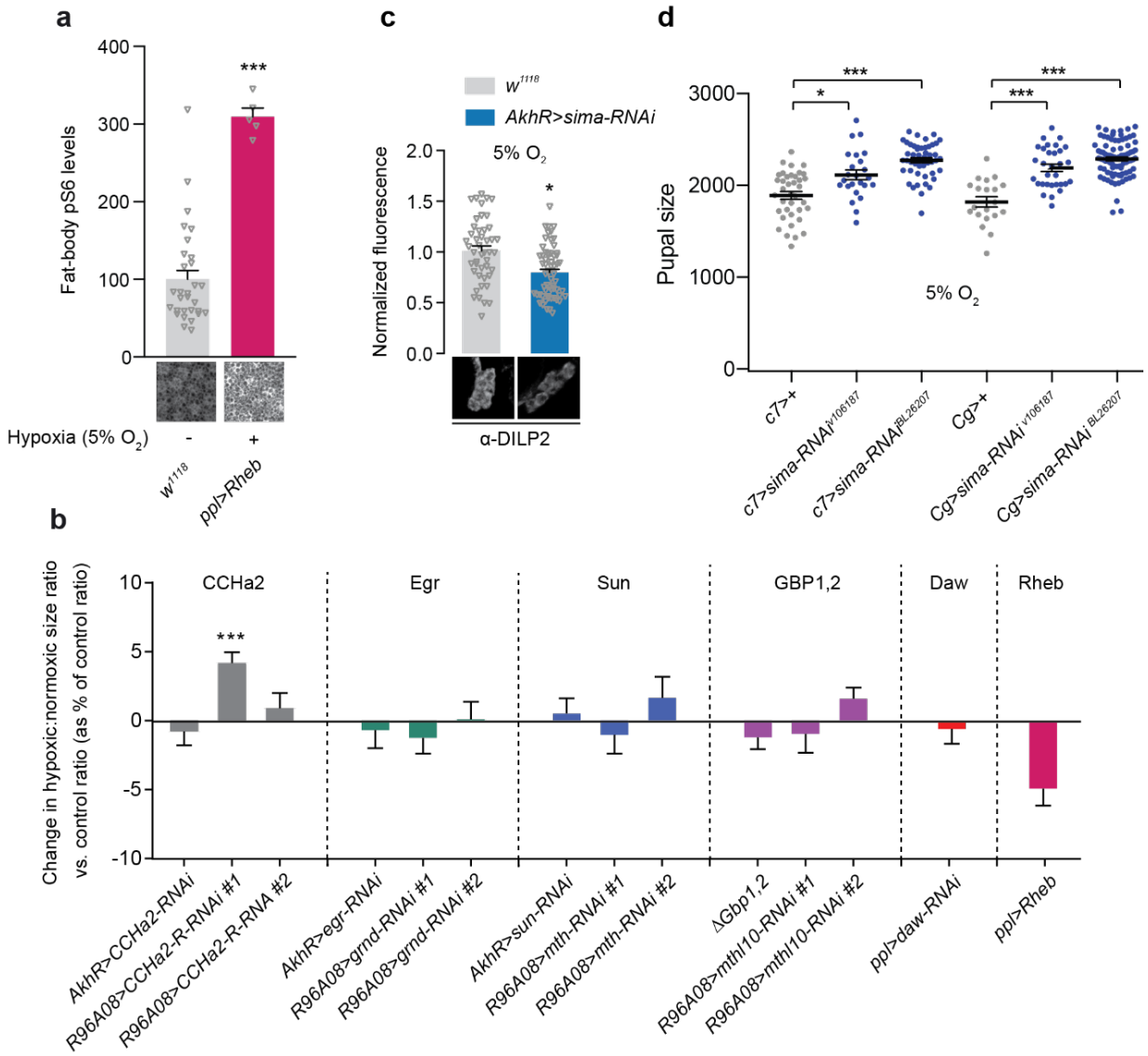

Supplementary Fig. 6. a Fat-body-specific expression of Rheb stimulates S6 phosphorylation under hypoxia, indicating increased Tor pathway activity. *n* = 5-30. **b** We conducted a mini-screen of known fat-body factors and IPC-expressed receptors for hypoxia-specific effects, hypothesizing that knocking down a factor or receptor that is involved in the insulinostatic response would rescue the size reduction (*i.e.*, lead to larger pupae) under hypoxia. *AkhR-GAL4::p65* (*AkhR>*) or *ppl-GAL4* (*ppl>*) drove RNAi against secreted factors and *Rheb* expression (inducing activation of Tor) in the fat body, while *R96A08-GAL4* (*R96A08>*) was used to knock down their respective receptors in the IPCs. Zero change indicates that an RNAi treatment had no hypoxia-specific effect – the ratio between hypoxic and normoxic sizes was the same as for controls. Roughly +20% would represent a complete blockage of hypoxia-induced size reduction. *CCHa2/CCHa2-R* results are inconsistent with each other, and a size increase upon *CCHa2-R* knockdown is inconsistent with its reported insulinotropic effects; thus perhaps the *CCHa2-R-RNAi-#1* phenotype reflects off-target effects. *n* = 1-14 vials (4-168 hypoxia:normoxia comparisons) per genotype. **c-d** Fat-body-specific *sima/HIF-1a* RNAi-mediated knockdown (mimicking the Tor-independent aspects of fat-body normoxia) reduces hypoxia-induced DILP2 retention (**c**) and partially rescues hypoxia-induced systemic body growth inhibition (**d**). c: *n* = 40-55. d: *n* =20-47. Statistics: two-tailed Student's t-test for pairwise comparisons versus controls. ***P<0.001, compared to the *Luciferase* control. Error bars indicate standard error of the mean (SEM). Underlying data are provided in the Source Data file.

Supplementary Table 1. Primers used in this study in qPCR assays.

Target gene	**Forward primer**	**Reverse primer**
branchless	TGCCCTATCACAGAGTTGC	ACCTACACGAACGCCATCAC
Dilp2	CTCAACGAGGTGCTGAGTATG	GAGTTATCCTCCTCCTCGAACT
Dilp3	CAACGCAATGACCAAGAGAAC	GCATCTGAACCGAACTATCACTC
Dilp5	ATGGACATGCTGAGGGTTG	GTGGTGAGATTCGGAGCTATC
Eip75B (E75B)	CAACAGCAACAACACCCAGA	CAGATCGGCACATGGCTTT
InR	CTCAGCCATACCAGGGACTTT	CTCTCCATAACACCGCCATC
RpL32	AGTATCTGATGCCCAACATCG	CAATCTCCTTGCGCTTCTTG